Journal of Molecular Structure 1117 (2016) 105–112

Contents lists available at ScienceDirect

Journal of Molecular Structure

journal homepage: http://www.elsevier.com/locate/molstruc

Theoretical investigation on local structure and transport properties of $NaF–AlF_3$ molten salts under electric field environment

Xiaojun Lv [a], Zhenming Xu [a], Jie Li [a, *], Jiangan Chen [b], Qingsheng Liu [c]

[a] School of Metallurgy and Environment, Central South University, Changsha 410083, China
[b] Faculty of Resource and Environmental Engineering, Jiangxi University of Science and Technology, Ganzhou 341000, China
[c] Faculty of Metallurgical and Chemical Engineering, Jiangxi University of Science and Technology, Ganzhou 341000, China

ARTICLE INFO

Article history:
Received 24 January 2016
Received in revised form
20 March 2016
Accepted 21 March 2016
Available online 24 March 2016

Keywords:
Molecular dynamics
Structure properties
Transport properties
$NaF–AlF_3$
Molten salts
Electric fields

ABSTRACT

The effect of electric field and molecular ratio CR (NaF/AlF_3) on basic structure and transport properties of $NaF–AlF_3$ molten salts were investigated by molecular dynamics simulations with the Buckingham potential model. The $[AlF_6]^{3-}$ groups are the dominant specie in $NaF–AlF_3$ molten salts at CR $\geq$ 2.6, and followed by the $[AlF_5]^{2-}$ groups, while CR $\leq$ 2.4, $[AlF_5]^{2-}$ groups are the protagonists up to 40%. In $NaF–AlF_3$ system, with the increase of CR, the proportion of F_b decreases slightly and the percentage of F_f increases dramatically. The Al–F bonds have ionic characters as well as partial covalently characters due to the hybridization of F-2p and Al-3s, 3p orbitals. The order of ion diffusion ability follows as $Na^+ > F^- > Al^{3+}$. Adding more NaF can break some F bridges of structure networks and decrease the polymerization degree of $NaF–AlF_3$ molten salts, the viscosity reduces and ionic conductivity increases as a consequence. The calculated results of ionic conductivity are in agreement with the experimental results. Electric field has no significant impact on the local structure characters, while transport properties are not. The change of CR (NaF/AlF_3) can significantly affect these characters of both the structure and transport.

1. Introduction

Deep understanding about the structure and transport properties of $[AlF_x]^{3-x}$ groups of $NaF–AlF_3$ molten salts has become an interesting issue, because its physical and chemical properties play key roles on the electro-deposition of Al metal from alumina in the industrial Hall–Heroult process [1,2]. In addition, a better knowledge of the structure and transport properties in $NaF–AlF_3$ molten salt systems is required for the correct interpretation of their spectroscopic data. For this reason, $NaF–AlF_3$ molten salts have been already investigated extensively both by theoretical simulations [3–6] and experiments [7–12]. Gilbert et al. have reproduced the structure properties and Raman spectra of several $NaF–AlF_3$ crystal compounds by using molecular dynamics (MD) simulations based on the rigid ionic (RI) model, and proposed that, only the tetrahedral $[AlF_4]^-$ groups exist in the molten salt of $NaAlF_4$ [9]. In 2014, Serpil Cikit pointed out the five-coordinated $[AlF_5]^{2-}$ and six-coordinated $[AlF_6]^{3-}$ groups are the dominant species in Na_3AlF_6 molten salt (cryolite) by the MD simulation [5]. Furthermore, some high temperature Raman [8,10,12] and NMR [7,9,13] experiments give an alternative experimental window to insight the evolution of the $[AlF_x]^{3-x}$ groups with different molten salt compositions. The predominance of $[AlF_5]^{2-}$ in cryolite molten salt, proposed by Serpil Cikit is consistent with the NMR data [7]. However, the experimental measurements on molten fluoride salt can be limited by its expensive cost and strong corrosion of fluoride salt. Fortunately, the computational simulation can provide a low cost method assisted with experiments to research the molten fluoride salts.

As we all know, $NaF–AlF_3$ molten salt of aluminum reduction serves in the electric field environment with a cell voltage about 4 V and current of 300–500 kA. While all the published works about the MD simulations of $NaF–AlF_3$ molten salts don't consider the effect of electric field environment [14,15], which is more closer to the truth and crucial for the deep research on the transport properties of $NaF–AlF_3$ molten salts. The MD simulations of Serpil Cikit's work [5] don't contain dipole–dipole attractive interaction between two atoms (equivalent to the Born-Mayer potential model) and only consider the coulomb and short-range repulsive interactions. The overlook of dipole–dipole attractive interaction

* Corresponding author.
E-mail address: 15216105346@163.com (J. Li).

http://dx.doi.org/10.1016/j.molstruc.2016.03.076
0022-2860/

may reduce the accuracy of describing the short-range structure of NaF–AlF_3 molten salts, such as bond length, angle length and CN. In addition, densities of NaF–AlF_3 molten salts within the work of Serpil Cikit et al. were fixed to the experimental values rather than predicted [5]. Being different from the Born-Mayer potential model, the Buckingham potential model allows a straightforward treatment of the dipole–dipole attractive interaction of atoms, which has been successfully applied in the fields of MD simulation of glass [16,17]. It can improve the accuracy of reproducing the short and medium-range structure of NaF–AlF_3 molten salts.

In this work, we carried out multi-scale simulations with molecular dynamics by the Buckingham potential model [18,19] and *ab* initio methods to enhance our knowledge of local structure and transport properties of NaF–AlF_3 molten salts under electric field environment. It is worth to notice that our work is the first to consider the electric field environment into MD simulation for NaF–AlF_3 molten salts. The effect of electric field and molecular ratio (CR, NaF/AlF_3) on basic structure-transport properties were calculated and compared with the experimental measurements to verify the MD model and potential parameters for NaF–AlF_3 molten salts.

2. Computational methods

2.1. Potential model

A key of molecular dynamics simulation is to choose an appropriate potential model and its corresponding parameters which are suitable for the calculation of particle interactions. In the common two-body potential model [18,19], there are three kinds of potential function: long-range coulomb interaction, short-range repulsion interaction and dipole–dipole attractive interaction. They have been generally and successfully used in MD simulation of the glass and ionic molten salts, and they were applied here:

$$V_{LR}^{ij}(r_{ij}) = \frac{q_i q_j}{4\pi\varepsilon_0}\frac{1}{r_{ij}} \quad (1)$$

$$V_{SR}^{ij}(r_{ij}) = A_{ij}\exp\left(-\beta_{ij}r_{ij}\right) - \frac{C_{ij}}{r_{ij}^6} \quad (2)$$

where the long-range potential, $V_{LR}^{ij}(r_{ij})$, in Eq (1) describe the coulomb interaction, which is defined for the interactions between two atoms, i and j. Here, q_i, ε_0 and r_{ij} donate the charge of ions, the dielectric constant in vacuum, and the distance between two particles, respectively. The short-range potential, $V_{SR}^{ij}(r_{ij})$, in Eq (2) works between the cation–cation, cation–anion and anion–anion pairs. We selected the Buckingham potential for the short-range potential, and A_{ij},β_{ij}, and C_{ij} are the potential parameters that determine the pair interactions between two particles.

The coulomb interactions act between all species, whereas the Buckingham potential model acts for the Na–F, Al–F, Al–Al, Na–Al and F–F short-range interactions. The charge of ions as this: Na = 0.72*e*, Al = 2.16*e*, F = −0.72*e*, which were obtained from our previous DFT calculations for a Na_3AlF_6 crystal cell. Table 1 lists all the force field parameters used in this work. It is worth highlighting that we derived, for the first time, a set of Buckingham parameters A_{ij},β_{ij}, and C_{ij} for all the atom pairs were independently fitted by the some data of potential energy vs interatomic distance, which were obtained by scanning the potential energy curve of different atom pairs, and the related details are listed in the electronic supplementary information.

Table 1
The Buckingham interatomic potential parameters.

Ions pair	A_{ij}[eV]	β_{ij}[Å]	C_{ij}[eV·Å^6]
Na–Na	0	1	0
Na–F	12230.42	4.28	90.89
Al–Al	9830.5	2.06	675
Na–Al	4929.05	3.22	0
Al–F	47181.82	5.48	22.75
F–F	24300.26	5.04	6.56

To test the validation of interatomic potential parameters, the lattice parameters of NaF, AlF_3 and Na_3AlF_6 crystals were reproduced and compared with the theoretical and experimental results [20], as shown in Table 2. As a whole, the lattice parameters of above crystal reproduced by the Buckingham potentials parameters are in good agreement with the theoretical and experimental results, whereas some deviation for AlF_3 crystals can be observed. It is important to emphasize the portability and accuracy of potential parameters in itself is a pair of contradiction, and the Al–Al pair potential is difficult to reproduce lattice parameters of AlF_3 and Na_3AlF_6 crystals simultaneously. In view of our work mainly focusing on the clusters of $[AlF_x]^{3-x}$, so the accuracy of Al–Al pair potential can be postponed.

2.2. Details of MD simulations

DL-POLY package was employed for our MD simulations. The Verlet Leap-Frog algorithm was used with a time step of 1fs to solve the equation of Newton motions. Ewald sums were used for all coulomb and multipolar interactions with a buffer width 0.5 Å and an accuracy of 10^{-5} kcal/mol [21–23]. The short-range interaction cutoff was set to 15 Å. Periodic boundary conditions were applied to all sides of the model box to create an infinite system with no boundaries, so that the calculation results would be more convincible. An external electric field was imposed and the ions were subjected to electric forces. We used a reasonable electric field $E = 0.1$ eV/Å (that is, 10^9 V/m; the unit of electric force acting on the elementary charge *e* is 1 eV/Å = 10^{10} V/m) in the X direction to obtain a detectable ion current but not to disturb the molten salt structure [15]. Initial configurations of 4000 ions for molecular dynamics were prepared by packing ions randomly in the simulation box in order to properly simulate the liquid state. Number of atoms of each molar compositions in the box of molten salts are shown in Table 3. To mix the system completely and eliminate the effect of the initial distributions, we heated the box system up to 4000 K in an NPT ensemble for 300 ps at 1.01 MPa, which means the simulations were run by keeping the number of particles (N), pressure (P) and the temperature (T) of the system constant. Then the hot liquid was cooled down at a rate of 1 K/ps to the melting point at 1283 K. Another 200 ps of equilibrium at NPT ensemble run is performed for relaxation. After these runs, convergence was achieved and the densities difference between the initial and final state were less than 1%. Finally, we collected the trajectories of atoms for the following statistical calculation of structure and transport properties.

2.3. Conditions of ab initio calculation

Density of states, electron density and Mulliken population calculations of the selected molecular clusters were performed with the dispersion-corrected DFT-D2 method [24], provided by the program package CASTEP [25]. The generalized gradient approximation (GGA) with the Perdew-Burke-Ernzerhof (PBE) exchange correlation potential was used [26]. Energy cutoff of 300 eV and a 1 × 1 × 1 *k*-point mesh were chosen to be used in this quantum chemical calculation. The ultrasoft pseudo potentials

Table 2
Comparison of predicted and experimental calculation lattice parameters for NaF, AlF_3 and Na_3AlF_6 crystals.

Species	Crystal structure	Space group	*a*(Å)	*b*(Å)	*c*(Å)
NaF	Cubic	$Fm\bar{3}m$	4.69(4.71[a])	4.69 (4.71[a])	4.69 (4.71[a])
AlF_3	Rhombohedral	$R\bar{3}c$	4.55(5.15[b])	4.55(5.15[b])	6.97(6.31[b])
Na_3AlF_6	Orthorhombic	*Immm*	5.57(5.4[c])	5.67(5.58[c])	7.98(7.76[c])

[a,b] Obtain by our DFT calculation.
[c]Ref. [20].

Table 3
Number of atoms of each molar compositions in the box of NaF–AlF_3 molten salts at 1 atm and 1283 K.

Number	Species	CR	n(NaF)	n(AlF_3)	Number of particles
NA1	Na_2AlF_5	2.0	1000	500	4000
NA2	$Na_{11}Al_5F_{26}$	2.2	1048	476	4000
NA3	$Na_{12}Al_5F_{27}$	2.4	1090	455	4000
NA4	$Na_{13}Al_5F_{28}$	2.6	1130	435	4000
NA5	$Na_{14}Al_5F_{29}$	2.8	1168	416	4000
NA6	Na_3AlF_6	3.0	1200	400	4000

(USPP) have been employed for all the ion–electron interactions. The ionic cores were represented by USPP for Na, Al and F atoms. The Na $2s^22p^63s^1$ electrons, Al $3s^23p^1$ electrons and F $2s^22p^5$ electrons were explicitly regarded as valence electrons. The geometry optimization parameters such as the maximum force was set to 0.01 eV/Å, the maximum stress to 0.02 GPa and the maximum displacement to 5.0×10^{-4} Å. The tolerance for the elastic constants calculation is set to 1×10^{-6} eV/atom, the maximum force to 0.002 eV/Å and the maximum displacement to 1.0×10^{-4} Å.

2.4. Statistics of structure information

The partial radial distribution function (PRDF) analysis was conducted from the MD trajectories to study the local structure in fluoride molten salts. The RDFs give the probability of finding an ion within a distance Δr from a specified particle at the location of r and the CNs show the average coordination number (CN) for atom i around atom j [27]. The equation of PRDF is expressed as below (Eq. (3)).

$$g_{ij}(r) = \frac{V}{N_i N_j} \sum_j \frac{\langle n_{ij}(r, \Delta r) \rangle}{4\pi r^2} \tag{3}$$

where, V is the volume of the MD box cell and N is the number of a special particle. n_{ij} (r, Δr) is the average number of atom j surrounding a central atom i within a defined cut-off distance Δr.

The first-shell coordination number (CN) of Al with the surrounding F anion was estimated by numerical integration of the PRDFs within the cut-off radius, which corresponds to the first minima of the corresponding partial $g_{Al\text{-}F}$ (r) [22]. We referred to the integral of the PRDF as the function (Eq. (4)),

$$N_{Al-F} = 4\pi\rho_F \int_0^R r^2 g_{Al-F}(r) dr \tag{4}$$

where $g_{Al\text{-}F}$ (r) is the PRDF between species Al and F, and ρ_F the average number density of species F atom.

2.5. Calculation of transport properties

Through statistical analysis of the particle trajectories, the function of mean square displacement (MSD) of time would be generated by the Einstein–Smoluchowshi equation [21].

$$\mathrm{MSD} = \langle \Delta\vec{r}(t)^2 \rangle = \frac{1}{N} \left\langle \sum \left| r_{i(t)} - r_{i(0)} \right| \right\rangle \tag{5}$$

where, $r_{i(t)}$ is the location of atom i at the time of t and the bracket means an ensemble average.

Combined with the knowledge of statistical thermodynamics, some transport properties of molten salts such as self-diffusion coefficient D of ions, viscosity η and ionic conductivity σ would be calculated according to the MSD curves of particles. The relation between the self-diffusion coefficient D of ions and the MSD curve is shown as below [28].

$$D = \lim_{t\to\infty} \frac{1}{6} \frac{d\left[\Delta r(t)^2\right]}{dt} \tag{6}$$

Then the viscosity η and ionic conductivity σ can be obtained by combining the self-diffusion coefficient D with the Einstein–Stokes formula and Nernst–Einstein equation respectively [29].

$$\eta = \frac{K_B T}{4\pi D\lambda} \tag{7}$$

$$\sigma = D\frac{nq^2}{K_B T} \tag{8}$$

where, K_B is the Boltzmann constant which equals to 1.38×10^{-23} J/K, T is the temperature of the system, λ is the step length of ion diffusion and it is generally considered to be equal to the diameter of ion ($\lambda = 2$ R), n presents the unit volume concentration of carrier atoms, and q is the charge of carrier atoms.

3. Results and discussions

3.1. Structure information

After MD simulation with electric field and none, the structural information was obtained from the statistical calculation of particles' trajectories. Fig. 1 show the local ionic structure of NaF–AlF_3 molten salts (NaF/AlF_3 = 3). The free F ions are represented by red balls, the Al complexes are represented by grey polyhedrons, and the Na^+ are represented by blue balls. In grey polyhedrons the bonds between Al and F ions represent that their distances are less than the first minimum of the radial distribution function. In this work, "bond" is not a real chemical bond but just an atom pair within a specified distance. Fig. 1b indicates that Na^+ ions prefer to distribute on the negative side of the electric field and the local ionic structure is governed by five-coordinated and six-coordinated Al species, corresponding to the distorted trigonal bipyramid and octahedral configuration. both in electric field environment and none. For NaF–AlF_3 molten salts, though losing long-range order, the local ion structure keeps the short-range order of five-coordinated $[AlF_5]^{2-}$ and six-coordinated $[AlF_6]^{3-}$.

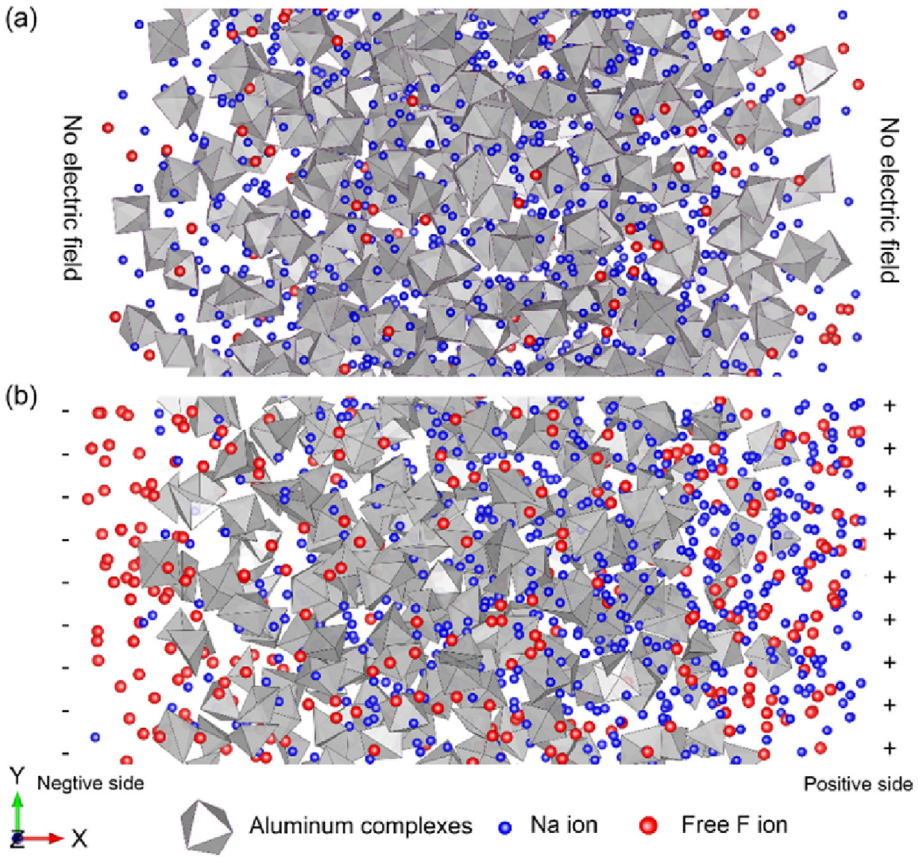

Fig. 1. Snapshot of the ion structure states in simulations of the cryolite composition ($NaF/AlF_3 = 3$), (a) with electric field; (b) without electric field; the right side is positive and the left is negative side.

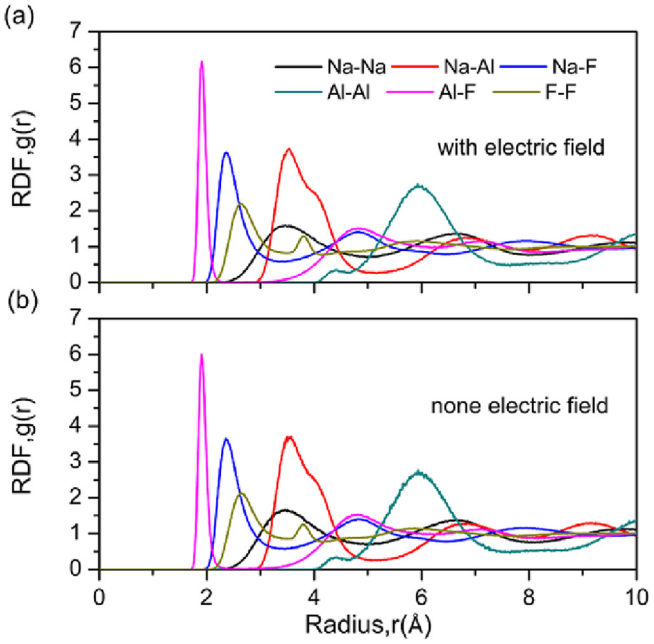

Fig. 2. Calculated Na–Na, Na–Al, Na–F, Al–Al, Al–F and F–F radial distribution functions in $NaF–AlF_3$ molten salt, CR = 3, (a) with electric field; (b) none electric field.

3.2. Radial distribution functions and coordination number

The partial radial distribution functions (RDFs) of $NaF–AlF_3$ molten salts with electric field and none are shown in Fig. 2. It can be seen from Fig. 2 that the first peak of Al–F is quite sharp, which indicates the F^- anions around Al^{3+} are arranged in the orderly states. Table 4 also summarizes the predicted local structure characters for ion pairs in $NaF–AlF_3$ molten salts from our MD simulations in comparison with other calculated values in the literatures [6,14,15]. With the integral of Al–F pair RDF, the average CN would be obtained and the ordinate value (special cutoff 2.4 Å) corresponding to the integral function is considered to be it. From Fig. 2 and Table 4, we observed that the electric field slightly increases all bond lengths except for F–F bond. The first peak of Al–Al located at 5.93 Å is much larger than twice that of the Al–F, indicating only a few Al–Al bonds existing in the molten salts are linked by bridging F^- anions.

As for a central Al^{3+} ion, the F^- anions are located at its first shell, the second shell is occupied by Na^+ ions, and the same Al^{3+} ions are in the third shell, indicating that the Coulomb forces dominate the interionic interactions for $NaF–AlF_3$ molten salts. The first-shell average coordination numbers (CN) of Al–F in $NaF–AlF_3$ molten salts are smaller than CN 6 of Na_3AlF_6 crystal and also increase a little under electric field environment at CR $\leq$ 2.4. The F–Al–F bond angles mainly distribute between 70° and 120°, and the peak values of F–Al–F bond angles and densities of $NaF–AlF_3$ molten salt obviously decrease with the employment of electric field.

The variation law of the influence of CR (NaF/AlF_3) on molten

Table 4
Comparison of the first-peak radius (in Å), first-shell average coordination number (CN) of ion pairs, peak of F–Al–F bond angle (in degree) and densities (in g/cm^3) of NaF–AlF_3 molten salts with other calculated values in the literatures. The calculated values of without electric field are listed in brackets.

	CR(NaF/AlF_3)							Ref [14]	Ref [15], ref [6]
	Ion pairs	2	2.2	2.4	2.6	2.8	3	CR = 2	CR = 3
First-peak radius	Na–Na	3.55(3.53)	3.57(3.52)	3.57(3.54)	3.55(3.52)	3.53(3.45)	3.53(3.5)	3.6	3.55, 3.65
	Na–Al	3.61(3.58)	3.53(3.51)	3.57(3.57)	3.57(3.55)	3.53(3.55)	3.53(3.49)	3.8	3.57, 3.66
	Na–F	2.37(2.36)	2.37(2.36)	2.37(2.36)	2.37(2.36)	2.37(2.37)	2.37(2.35)	2.2	2.2,2.24
	Al–Al	3.85(3.78)	3.85(3.83)	3.89(3.96)	4.01(3.96)	3.93(3.93)	3.9(3.88)	4.0	3.59, 3.74
	Al–F	1.89(1.88)	1.89(1.88)	1.89(1.89)	1.91(1.9)	1.91(1.89)	1.91(1.9)	2.0	1.81, 1.78
	F–F	2.67(2.67)	2.65(2.65)	2.67(2.66)	2.65(2.66)	2.65(2.66)	2.63(2.64)	2.8	2.52, 2.54
Al^{3+} CN	Al–F	5.09(5.06)	5.31(5.23)	5.5(5.49)	5.72(5.7)	5.83(5.88)	5.98(6.02)	6.25	6.4, 5.9
Bond angle	F–Al–F	86(87)	89(88)	84(89)	81(85)	85(89)	86(89)	85	
Density		1.92(1.92)	1.99(2.0)	2.06(2.09)	2.14(2.17)	2.19(2.23)	2.25(2.28)	1.99	

salts local ionic structure is inconsistent, the average bond lengths of Na–Na, Na–Al, F–F decrease and Al–F increase with the increase of CR. But the Na–F bond length is not affected by CR. In addition, when improving the CR of molten salts, the average number of F^- anions around a central Al^{3+} cation in the first-shell increase and the ionic structure of molten salt change to compactness, so the densities of NaF–AlF_3 molten salts system become larger.

Compared with other people's calculated values, the results of our MD simulations have some difference with them. It may be because the additional dipole–dipole attractive interaction were considered into our MD simulations, which may improve the simulated results. Moreover, all densities of NaF–AlF_3 molten salts systems in the literatures [6,14,15] were fixed to experimental values rather than predicted, so they can't demonstrate the inaccuracy of our MD simulated results. In Section 2, our potentials model and parameters have reproduced structure properties for Na_3AlF_6 crystals successfully and the results are in good agreements with the theoretical and experimental data. What is noteworthy is that there is few experimental results of the average bond length and bond angles of NaF–AlF_3 molten salts for comparison. We hope our calculated results can motivate future experimental work to verify them.

3.3. Distributions of CN and F atom types

The distribution of coordination numbers was obtained by calculating the percentage of an Al^{3+} ion having a given number of neighbors (F^- anions) from all the trajectories of MD simulation. Neighbors are these ions which are located inside the first shell corresponding to the position of the minimum of the PRDF illustrated in Fig. 2. Fig. 3a shows the percentage of Al^{3+} ions which were four-coordinated, five-coordinated, or six-coordinated structures and the F atom types at the different compositions and electric field environment. It is observed that an important and special ionic structure at CR 2.4–2.6 is the boundary of variation law. The $[AlF_6]^{3-}$ groups are the dominant species about 50% in NaF–AlF_3 molten salts at CR $\geq$ 2.6, corresponding to octahedral symmetry. The results given in Fig. 3a agree with those deduced from the experimental Raman spectrum, asserting that six-coordinated $[AlF_6]^{3-}$ groups are the major species in molten cryolite [30]. While CR $\leq$ 2.4, five-coordinated $[AlF_5]^{2-}$ groups are the protagonists up to 38–40% in the molten salts, and the percentage of $[AlF_6]^{3-}$ and $[AlF_4]^-$ lie in 30–35%. Besides, as a whole, with the increase of CR, some $[AlF_4]^-$ and $[AlF_5]^{2-}$ groups dissociate from the $[AlF_6]^{3-}$ groups, so the percentages of $[AlF_6]^{3-}$ decrease and $[AlF_4]^-$, $[AlF_5]^{2-}$ groups increase as a consequence. The electric field environment makes some $[AlF_6]^{3-}$ dissolve to $[AlF_4]^-$, $[AlF_5]^{2-}$ groups at CR $\geq$ 2.6, while some $[AlF_4]^-$, $[AlF_5]^{2-}$ groups turn into the $[AlF_6]^{3-}$ groups at CR $\leq$ 2.4.

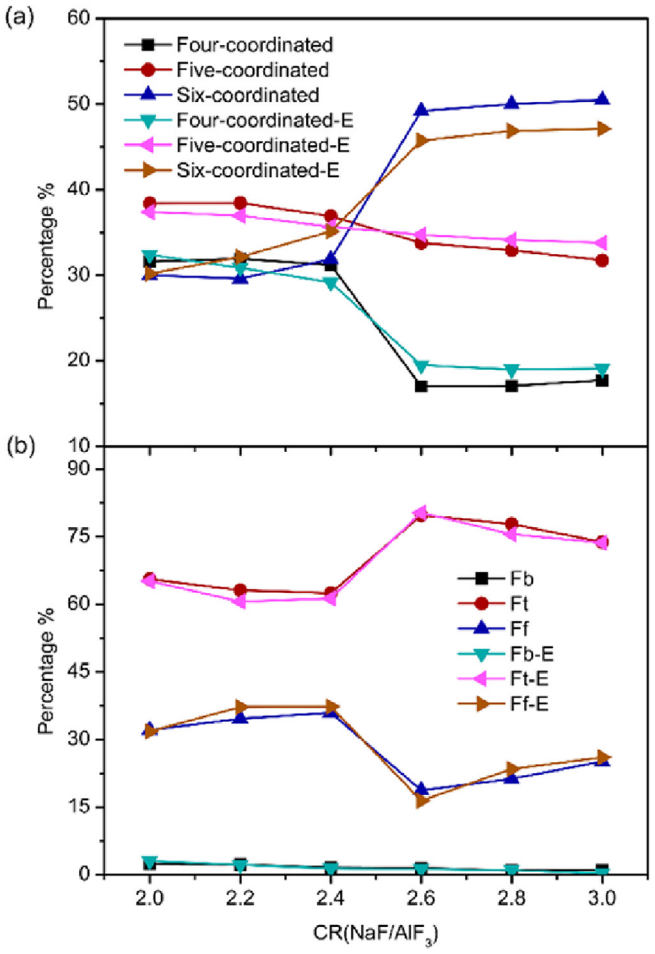

Fig. 3. Distribution of coordination numbers and F atom types in different CR (NaF/AlF_3) under electric field environment and none.

The F atom types (bridging F_b, terminal F_t and free F_f) measure the structure polymerization degree of NaF–AlF_3 molten salts and has a significant impact on the transport properties. In Fig. 3b, it can be seen that, in NaF–AlF_3 system, the percentage of F_b is small about 1–3%, which indicates the polymerization of ionic structure is not conspicuous and the fluidity of these NaF–AlF_3 molten salts is excellent. It is consistent with the fact the first peak of Al–Al pair's PRDF located at 5.93 Å is much larger than twice that of the Al–F. When CR $\geq$ 2.6 or CR $\leq$ 2.4, with the increase of CR, the proportion of F_b and F_t decreases slightly and the percentage of F_f increases dramatically. This is due to the reason that Al ion has a tendency to

form $[AlF_6]^{3-}$ groups, making some F^- anions act as bridges to connect two Al^{3+} cations and arousing the polymerization of NaF–AlF_3 molten salts structure. F_t is the prominent F atom type, which is up to 60–80% in different components of NaF–AlF_3 molten salts. Furthermore, the electric field environment has no significant effect on the distribution of F atom types.

3.4. Electronic structure of the $[AlF_6]^{3-}$ cluster

In NaF–AlF_3 molten salts system, the $[AlF_6]^{3-}$ cluster is the dominant species according to our MD simulations. To insight the electronic structure properties such as density of states, electron density and Mulliken populations, we carried out the quantum chemical calculations for the selected $[AlF_6]_4$ Na_{12} cluster from a certain MD trajectory. In a typical cluster of $[AlF_6]_4Na_{12}$, the central $[AlF_6]^{3-}$ complex is surrounded by a second solvation shell with a total of three Na^+ ions. Total and partial density of states (DOS) of a $[AlF_6]_4Na_{12}$ cluster were obtained, as shown in Fig. 4. The electron orbitals near core with lowest energy around −50 eV were occupied by Na-3s states and electron orbitals with middle energy around −20 eV were occupied by Na-2p and F-2s states. In addition, the electron orbitals near the Fermi (HOMO) level is essentially dominated by F-2p states, with an admixture with Al-3s, 3p states. It indicates some covalent bonding interactions (Al–F) exist in the $[AlF_6]^{3-}$ cluster and the possibility of electrons to transit from Al-3s, 3p to F-2p states. Fig. 5 shows the electron density of a $[AlF_6]_4Na_{12}$ cluster, the electrons transferring from the central Al atoms and surrounding Na atoms are mainly localized at F atoms, implying the distinct Coulomb interactions exist in the $[AlF_6]_4Na_{12}$ cluster.

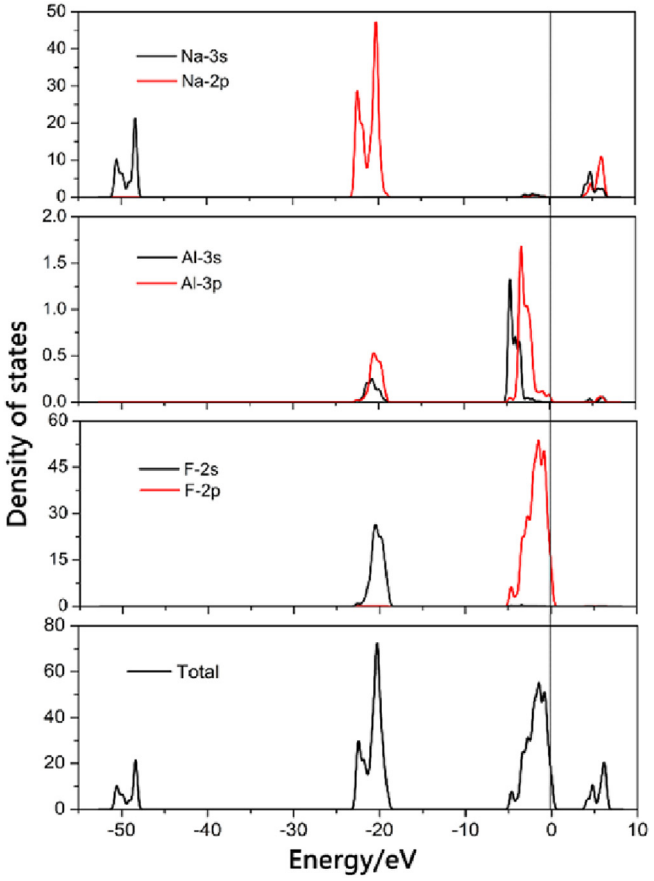

Fig. 4. Total and partial density of states (DOS) of a $[AlF_6]_4$ Na_{12} cluster. The vertical line indicates the Fermi (HOMO) energy.

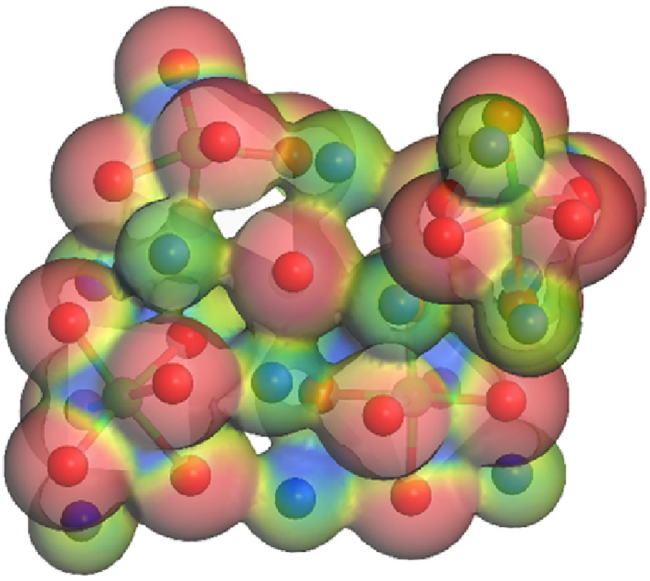

Fig. 5. Electron density of a $[AlF_6]_4$ Na_{12} cluster. Insert: The central $[AlF_6]^{3-}$ ion cluster.

Averaged Mulliken populations of the $[AlF_6]_4$ Na_{12} cluster are displayed in Table 5. The bond population of Al–F is 0.27, which is greater than the value of 0.035 of Na–F bond, implying the covalently character of the former is more evident than the latter. It is characteristic for Al–F bonds having ionic characters as well as partial covalent characters due to the hybridization of F-2p and Al-3s (3p) orbitals, while the Na–F and F–F bonds are ionic characters. It is in good agreement with the results of above density of states (DOS) analysis.

3.5. Transport properties

With the computational methods in Section 2.5, the MSD cures of NaF–AlF_3 molten salts of various compositions with electric field and none were obtained. One sixth of the slope of MSD cure in the linear region represents the ion's self-diffusion coefficients, and results were shown in Fig. 6. Then viscosity η was obtained by combining the self-diffusion coefficients D of all Na^+, Al^{3+}, F^- ions and Einstein–Stokes approximation, and the step length λ of ion diffusion was considered to be equal to the diameter of Na^+, Al^{3+}, F^- ion (so λ = 2.04, 1.07 and 2.66 Å). NaF–AlF_3 molten salts have a relatively high self-diffusion coefficient, so they have outstanding liquidity and ionic conductivity. Ionic conductivity σ was calculated by self-diffusion coefficients D and the Nernst–Einstein approximation. Our calculated results of viscosity η and ionic conductivity σ compared with the experimental values at 1300 K in these literatures [15,31–33] and our Factsage thermodynamic calculation were presented in Fig. 7.

It can be observed from Fig. 6 that the order of ion diffusion ability was found to be $Na^+ > F^- > Al^{3+}$ at any CR and with electric field environment or not. Electric field and CR (NaF/AlF_3) have a

Table 5
Average Mulliken atomic orbital populations (s, p), total population (Total), charges transferred (Charge) and overlap population of $[AlF_6]_4$ Na_{12} Cluster (unit: e).

Atoms	s	p	Total	Charges	Bonds	Population
Na	2.12	6.04	8.16	0.84	Na–F	0.035
Al	0.46	0.76	1.21	1.79	Al–F	0.27
F	1.96	5.76	7.72	−0.72	F–F	−0.03

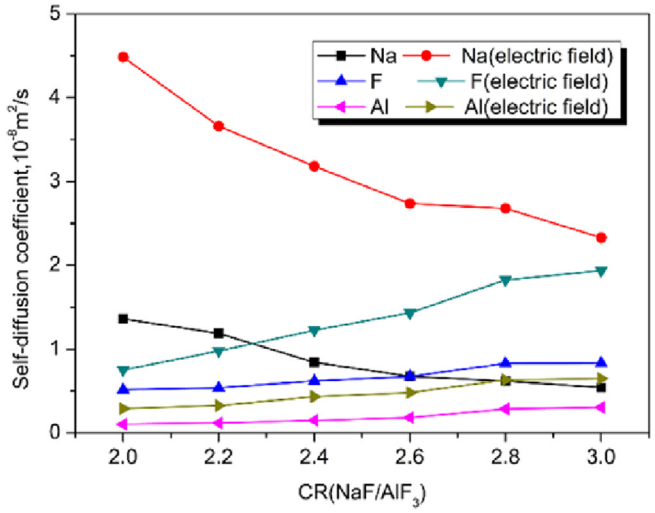

Fig. 6. Ion self-diffusion coefficients in different CR (NaF/AlF$_3$) and electric field environment.

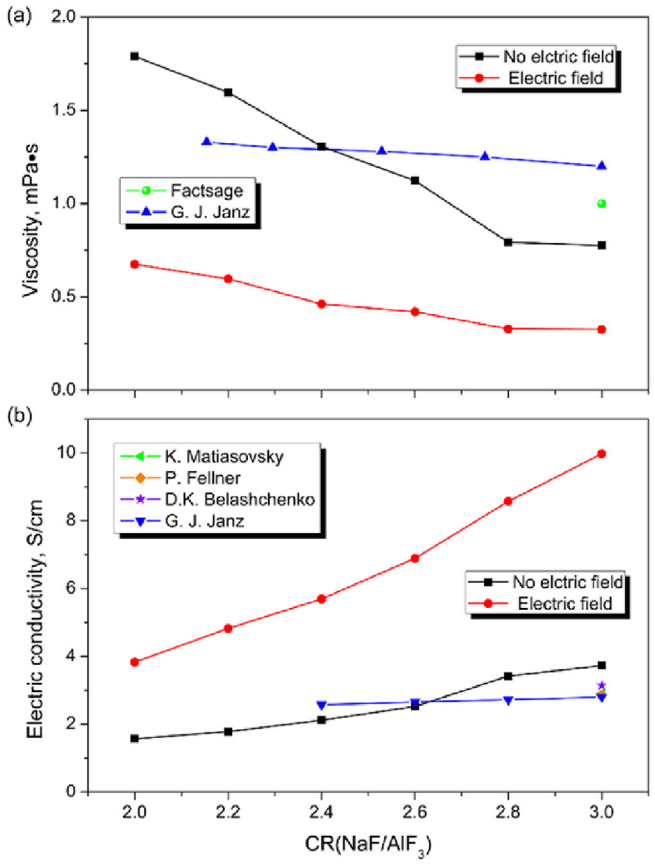

Fig. 7. Viscosity (a) and ionic conductivity (b) of NaF–AlF$_3$ molten salts with an electric field or not of various CR compared with the experimental values in literatures and Factsage thermodynamic calculation.

significant impact on the mobility of Na^+, Al^{3+} and F^- ions. Compared to the results without electric field, the mobility of Na^+ ions is enhanced by quadruple with electric field environment. Moreover, the mobility of Na^+ ions decreases with the increase of CR (NaF/AlF$_3$), but the mobility of Al^{3+}, F^- ions conversely increases. Combining above analysis of local ionic structures, adding more NaF can break some F bridge of structure networks and decreases the polymerization degree of NaF–AlF$_3$ molten salts, and the viscosity η reduces and ionic conductivity σ increases accordingly as a consequence, as shown in Fig. 7. It is obvious that the viscosity η of NaF–AlF$_3$ molten salts is mainly determined by the Al^{3+}, F^- ions having poor mobility.

Fig. 7a shows the change trend of calculated viscosity without electric field are in agreement with the experimental results of G. J. Janz [31]and our Factsage thermodynamic calculations. While the calculated results of viscosity η under electric field environment have some difference from them. As for the ionic conductivity σ of NaF–AlF$_3$ molten salts demonstrated in Fig. 7b, our calculated results without electric field are in good agreement with the experimental and theoretical calculation data [15,31–33] in spite of some negligible deviation, generally within 19%. When the MD simulations under electric field environment, some prominent difference were observed between these calculated results and experimental values. However, both experimental data and our calculated values with electric fields do not have any comparability, it is due to that these viscosity results measured in the experiments have no electric field and the difficulty of experimental measurements under high temperature may cause a certain errors of the viscosity and ionic conductivity data.

The deviations of viscosity between calculated and experimental results imply that the MD simulation of transport properties are fastidious about the potential parameters. The computational accuracy and efficiency is a pair of contradiction in the classical MD simulations. Therefore, we will carry out the *ab* initio molecular dynamics (AIMD) simulation of NaF–AlF$_3$ molten salts in the future works, which is flexible to study any system without needing to firstly fit potential parameters to experimental or computed values and improve the accuracy of the calculation. In view of our calculated ionic conductivity is in good agreement with experimental values, generally within 19%, the conclusion can be made that our MD simulations for structure and transport properties of NaF–AlF$_3$ molten salts are reliable. In sum, the electric field environment has no significant impact on the local structure characters of MD simulations, while the transport properties are not. The change of CR (NaF/AlF$_3$) can significantly affect the characters of both local structure and transport.

4. Conclusions

MD simulations under electric field environment with the Buckingham potential model and quantum chemistry calculations were carried out to enhance knowledge of key structure and transport properties of NaF–AlF$_3$ molten salts. The effect of electric field and molecular ratio CR (NaF/AlF$_3$) on basic structure-transport properties were studied and compared with the experimental results to verify the MD simulations of NaF–AlF$_3$ molten salts.

The local ionic structure characters of NaF–AlF$_3$ molten salts are governed by five-coordinated and six-coordinated Al species both in electric field environment and none. For NaF–AlF$_3$ molten salts, though losing long-range order, the local ion structure keeps the short-range order of five-coordinated $[AlF_5]^{2-}$ and six-coordinated $[AlF_6]^{3-}$. The electric field slightly increases all bond lengths except for F–F bond. First-shell average coordination number of Al–F increases a little under the electric field environment at CR $\leq$ 2.6. The bond length of Na–Na, Na–Al, F–F decreases and Al–F increases with the increase of CR, while the Na–F bond length is not affected by the CR. $[AlF_6]^{3-}$ groups are the dominant species in NaF–AlF$_3$ molten salts at CR $\geq$ 2.6, and followed by the $[AlF_5]^{2-}$ groups, while CR $\leq$ 2.4, $[AlF_5]^{2-}$ groups are the protagonists up to 38–40%. In NaF–AlF$_3$ system, with the increase of CR, the proportion of F_b decreases slightly and the percentage of F_f increases dramatically. It

is due to Al ion has a tendency to form $[AlF_6]^{3-}$ groups, making some F atoms act as bridges of networks and arousing the polymerization of NaF–AlF_3 molten salts structure. According to quantum chemical calculations, Al–F bonds of the $[AlF_x]^{3-x}$ groups in NaF–AlF_3 molten salts have ionic characters as well as partial covalently characters due to the hybridization of F-2p and Al-3s (3p) orbitals, while the Na–F and F–F bonds are ionic characters. The order of ion diffusion ability follow as $Na^+ > F^- > Al^{3+}$. The movement ability of Na, Al, F ions is enhanced by electric field. Adding more NaF can break some F bridges of structure networks and decreases the polymerization degree of NaF–AlF_3 molten salts, the viscosity reduces and ionic conductivity increases accordingly. Our calculated results of ionic conductivity are in good agreement with the experimental results, generally within 19%. In sum, the electric field has no significant impact on the structure characters, while transport properties are not. The change of CR (NaF/AlF_3) can significantly affect the characters of both structure and transport.

Acknowledgments

We sincerely acknowledge the High Performance Computing Center of CSU, China. This work was financially supported by the National Science and Technology Support Project of China (No. 2012BAE08B02) and National Natural Science Foundation of China (No. 51264011).

Appendix A. Supplementary data

Supplementary data related to this article can be found at http://dx.doi.org/10.1016/j.molstruc.2016.03.076.

References

[1] W.B. J, Aluminum production paths in the new millennium, JOM 51 (1999) 24.
[2] J.W. E, The evolution of technology for light metals over the last 50 years: Al, Mg, and Li, JOM 59 (2007) 30.
[3] R.R. Nazmutdinov, T.T. Zinkicheva, S.Y. Vassiliev, D.V. Glukhov, G.A. Tsirlina, M. Probst, A spectroscopic and computational study of Al(III) complexes in sodium cryolite melts: ionic composition in a wide range of cryolite ratios, Spectrochim. Acta A Mol. Biomol. Spectrosc. 75 (2010) 1244–1252.
[4] R.R. Nazmutdinov, T.T. Zinkicheva, S.Y. Vassiliev, D.V. Glukhov, G.A. Tsirlina, M. Probst, A spectroscopic and computational study of Al(III) complexes in cryolite melts: effect of cation nature, Chem. Phys. 412 (2013) 22–29.
[5] S. Cikit, Z. Akdeniz, P.A. Madden, Structure and Raman spectra in cryolitic melts: simulations with an ab initio interaction potential, J. Phys. Chem. B 118 (2014) 1064–1070.
[6] Lv Xiaojun, Xu Zhenming, Li Jie, Chen Jiangan, Liu Qingsheng, First-principles molecular dynamics investigation on Na3AlF6 molten salt, J. Fluorine. Chem 185 (2016) 42–47.
[7] E. Robert, V. Lacassagne, C. Bessada, D. Massiot, B. Gilbert, J.-P. Coutures, Study of NaF-AlF_3 melts by high temperature NMR spectroscopy: comparision with results from Raman spectroscopy, Inorg. Chem. 38 (1999) 214–217.
[8] B.M. Gilbert, T, Reinvestigation of molten fluoroaluminate Raman spectra: the question of the existence of AlF_5^{2-} ions, Appl. Spectrosc. 44 (1990) 299–305.
[9] B.R. Gilbert, E, E. Tixhon, J. Olsen, T. Ostvold, Structure and thermodynamics of NaF-AlF_3 melts with addition of CaF_2 and MgF_2, Inorg. Chem. 35 (1996) 4198–4210.
[10] X. w Hu, J. y Qu, B. l Gao, Z. n Shi, F. g Liu, Z. w Wang, Raman spectra of ionic structure for acidic NaF-AlF_3 melts, Chin. J. Nonferrous Metals 18 (2008) 1914–1919.
[11] T. Zhao, J. l You, Y. y Wang, L. Wang, L. Ma, Characteristic Raman spectra and quantum chemistry ab initio calculation on aluminum-fluorine tetrahedral model clusters of NaF-AlF_3 binar, Chin. J. Light Scatt. 24 (2012) 1–6.
[12] S. j Dai, Y. y Wang, W. Wang, Z. c Wang, Y. j Niu, Study of micro structure and Raman spectroscopic characteristics of sodium aluminum tetraf luoride, Chin. J. Light Scatt. 22 (2010) 276–280.
[13] V. Lacassagne, C. Bessada, P. Florian, S. Bouvet, B. Ollivier, J.-P. Coutures, D. Massiot, Structure of high-temperature NaF-AlF_3-Al_2O_3 melts: a multinuclear NMR study, J. Phys. Chem. B 106 (2002) 1862–1868.
[14] H. Hou, G. X, S. Chen, X. Zhang, Structure of molecular dynamics stimulated NaF-AlF_3 melts, Chin. J. Nonferrous Metals 10 (2000) 914–917.
[15] D.K. Belashchenko, O.I. Ostrovski, S.Yu. Saposznikova, Computer study of structure, thermodynamic, and electrical transport properties of $Na3AlF_6$-Al_2O_3 and CaF_2-Al_2O_3 melts, Metallurgical Mater. Trans. B 29B (1998) 105–110.
[16] P. Zhang, W. Hui, Y. Zhang, X. Ren, D. Zhang, Molecular dynamics simulation for the rapid solidification process of MgO–Al_2O_3–SiO_2 glass–ceramics, J. Non·Cryst. Solids 358 (2012) 1465–1473.
[17] G. Malavasi, A. Pedone, M.C. Menziani, Study of the structural role of gallium and aluminum in 45S5 bioactive glasses by molecular dynamics simulations, J. Phys. Chem. B 117 (2013) 4142–4150.
[18] E. Gambuzzi, A. Pedone, On the structure of Ce-containing silicophosphate glasses: a core-shell molecular dynamics investigation, Phys. Chem. Chem. Phys. 16 (2014) 21645–21656.
[19] T. Kitamura, Y. Umeno, F. Shang, T. Shimada, K. Wakahara, Development of interatomic potential for Pb(Zr, Ti)O_3 based on shell model, J. Solid Mech. Mater. Eng. 1 (2007) 1423–1431.
[20] B.J. K, Q. Zhou, High-temperature powder synchrotron diffraction studies of synthetic cryolite Na_3AlF_6, J. Solid. State. Chem. 177 (2004) 654–659.
[21] N. de Koker, Structure, thermodynamics, and diffusion in $CaAl_2Si_2O_8$ liquid from first-principles molecular dynamics, Geochim. Cosmochim. Acta 74 (2010) 5657–5671.
[22] F.J. Spera, M.S. Ghiorso, D. Nevins, Structure, thermodynamic and transport properties of liquid $MgSiO_3$: comparison of molecular models and laboratory results, Geochim. Cosmochim. Acta 75 (2011) 1272–1296.
[23] F.J. Spera, D. Nevins, M. Ghiorso, I. Cutler, Structure, thermodynamic and transport properties of $CaAl_2Si_2O_8$ liquid. Part I: molecular dynamics simulations, Geochim. Cosmochim. Acta 73 (2009) 6918–6936.
[24] J. Klimeš, D.R. Bowler, A. Michaelides, Van der Waals density functionals applied to solids, Phys. Rev. B 83 (2011).
[25] G. Kresse, Efficient iterative schemes for ab initio total-energy calculations using a plane-wave basis set, Physcal Rev. B 54 (1996) 169–186.
[26] K.B. John, P. Perdew, Matthias Ernzerhof, Generalized gradient approximation made simple, Phys. Rev. Lett. 77 (1996) 3865–3868.
[27] J.M. Ziman, Principles of the Theory of Solids, Cambridge University, Cambridge University Press, 1972.
[28] R. Kubo, The fluctuation-dissipation theorem, Rep. Prog. Phys. 29 (1966) 255–284.
[29] T. Wu, S. He, Y. Liang, Q. Wang, Molecular dynamics simulation of the structure and properties for the CaO–SiO_2 and CaO–Al_2O_3 systems, J. Non·Cryst. Solids 411 (2015) 145–151.
[30] Z.M. Akdeniz, P. A, Raman spectra of ionic liquids: a simulation study of AlF_3 and its mixtures with NaF, J. Phys. Chem. B 110 (2006) 6683–6691.
[31] G.J. Janz, R.P.T. Tomkins, Molten salts: volume 5, part 2. Additional single and multi-component salt systems. Electrical conductance, density, viscosity and surface tension data, J. Phys. Chem. Ref. Data 5 (1983) 591–815.
[32] P. Fellner, O. Kobbeltvedt, Å. Sterten, J. Thonstad, Electrical conductivity of molten cryolite-based binary mixtures obtained with a tube-type cell made of pyrolytic boron nitride, Electrochim. Acta 38 (1993) 589–592.
[33] M.M.a.S.O, K. Matiasovsky, Electrical conductivity of the melts in the system $Na3AlF_6$-Al_2O_3-NaCl, J. Electrochem. Soc. 111 (1964) 973–976.